Nature and Science of Sleep

Dovepress
open access to scientific and medical research

Open Access Full Text Article

ORIGINAL RESEARCH

Topological Regularization of Networks in Adult Patients with Moderate-to-Severe Obstructive Sleep Apnea-Hypopnea Syndrome: A Structural MRI Study

This article was published in the following Dove Press journal:
Nature and Science of Sleep

Wanqing Liu[1]
Chuanlong Cao[2]
Bing Hu[1]
Danyang Li[1]
Yumei Sun[1]
Jianlin Wu[1]
Qing Zhang[1]

[1]Department of Radiology, Affiliated Zhongshan Hospital of Dalian University, Dalian 116001, People's Republic of China; [2]Department of Radiology, Affiliated Xinhua Hospital of Dalian University, Dalian 116001, People's Republic of China

Objective: Patients with obstructive sleep apnea-hypopnea syndrome (OSAHS) exhibit neurocognitive impairments; however, the neuroimaging mechanism of neurocognitive impairments remains unclear. The aim of this study was to understand the neuroimaging mechanism in adult patients with moderate-to-severe OSAHS, from the perspective of the connectome.

Patients and Methods: Thirty-one untreated patients with moderate-to-severe OSAHS (mean age: 41.23±8.22) were compared with 26 good sleepers (GS) (mean age: 39.50±7.92) matched according to age, gender, handedness, and education level. All subjects underwent thin-slice T1WI scanning of the skull using a 3.0T MRI. Then, a large-scale structural covariance network was constructed based on the gray matter volume extracted from the structural MRI. Graph theory was then used to determine the topological changes in the structural covariance network of OSAHS patients.

Results: Although small-world networks were retained,the structural covariance network exhibited topological irregularities in regular architecture as evidenced by an increase in the clustering coefficient (p=0.009), transfer coefficient (p=0.029) and local efficiency (p=0.031), and a local increase in the shortest path length (p<0.05) compared with the GS group. Locally, OSAHS patients showed a decrease in nodal betweenness and degree in the left inferior parietal gyrus, left angular gyrus and right anterior cingulate cortex compared with the GS group (p<0.05, uncorrected). In addition, the resistance of structural covariance networks in OSAHS patients to random fault is significantly lower than that of the GS group (p=0.044).

Conclusion: Structural covariance networks are abnormal in terms of multiple network parameters, which provide network-level insight into the neuroimaging mechanism of cognitive impairments in adult OSAHS patients.

Keywords: obstructive sleep apnea-hypopnea syndrome, cognitive impairment, connectome, graph theory, gray matter volume

Introduction

Obstructive sleep apnea-hypopnea syndrome (OSAHS) is a sleep-related breathing disorder characterized by recurrent episodes of partial or complete obstruction of the upper airway during sleep. OSAHS often results in frequent insufficient ventilation or apnea, which ultimately leads to hypoxemia, hypercapnia, hemodynamic fluctuations and sleep breakdown.[1] The prevalence of OSAHS is about 2–4% in

Correspondence: Qing Zhang
Department of Radiology, Affiliated Zhongshan Hospital of Dalian University, No. 6, Jiefang Street, Zhongshan District, Dalian, Liaoning, People's Republic of China
Email zhangqingsmile@163.com

middle-aged men[2] and >50% in adults over the age of 65.[3] This disease severely affects the quality-of-life and safety of patients and causes memory loss, decreased work efficiency, daytime sleepiness and accident-proneness,[4] and may be associated with hypertension,[5] cardiovascular disease,[6] diabetes,[7] stroke[8] and Alzheimer's disease.[9] OSAHS patients also show neurocognitive deficits in attention, memory, learning ability, executive function, visual space function, and language skills,[10–12] but the neuroimaging mechanism of these neurocognitive impairments remains unclear.

Previous studies using magnetic resonance imaging (MRI) have confirmed significant gray matter differences in OSAHS patients; however, the results have varied significantly across studies.[13–15] Although most of these findings support the idea of gray matter atrophy in multiple regions of the brain occurs in OSAHS patients, especially in the marginal system,[16–18] some studies do not report any brain gray matter atrophy,[19] and a few studies have even found gray matter hypertrophy.[20] These conventional studies were able to determine changes in gray matter volume in multiple regions of the brain in OSAHS patients, however, these studies could not analyze the structural or functional relationship between such brain regions and interpret the changes at the whole-brain network level. In order to raise awareness of the complex network of the human brain, Sporns et al[21] proposed the concept of the human connectome to meticulously describe the organizational patterns within the brain. The brain is a complex continuum of neurons that are interconnected with one other and is no longer treated as a large number of discrete anatomical units or assemblies of chemical substances. This change of view will provide a new perspective for further in-depth exploration of the neurological activities within the brain and the pathogenesis of various neuropsychiatric disorders.

Graph theory is currently the standard method used to identify and characterize human brain networks. The graph theory approach describes the human brain network as a graph consisting of a set of nodes (neurons, brain regions) and a set of edges (structural or functional connections). Previous studies have demonstrated that although the structural and functional brain networks of OSHAS patients conform to the small-world characteristics, the network topology attributes change abnormally in OSHAS patients compared to healthy subjects. Park et al.[22] constructed brain functional networks in OSAHS patients for the first time using graph theory based on the resting-state functional MRI data. They observed that the global efficiency of OSHAS patients was significantly decreased and that the nodal properties were reduced in the whole brain. These results suggest that alterations in the network topology may be the cause of impaired responses in the autonomic nervous system, and cognitive and sensorimotor functions. Chen et al.[23–25] used graph theory to construct a resting-state functional network in OSAHS patients and found that the whole-brain functional network of OSAHS patients converged on to small-world characteristics, however, the small-world index, normalized clustering coefficient, and global efficiency decreased significantly, whereas the normalized shortest path increased. Luo et al.[26] used graph theory to construct a structural covariance network in children with OSAHS based on gray matter volume. The authors found that the local efficiency was reduced; the degree was decreased in the left corner gyrus, and the betweenness was reduced in the right lingual gyrus and the inferior frontal gyrus. These studies reveal changes in the topological properties of the OSAHS functional network in adults and the structural covariance network in children, however, the changes in the structural covariance network in adults with moderate-to-severe OSAHS remain unclear.

To this end, we used graph theory to analyze the changes in the topological properties of structural covariance networks in OSAHS adults. We further explored the neuroimaging mechanism in OSAHS patients with cognitive impairment reveal new imaging evidence for the OSAHS-based cognitive impairment.

Patients and Methods

Participants

This study was approved by the Ethics Committee of the Affiliated Zhongshan Hospital of Dalian University, and all participants provided written informed consent prior to participation in this study. Participants were recruited from July 2017 to November 2018 from the Department of Otolaryngology, Affiliated Zhongshan Hospital of Dalian University and the local community. All subjects were examined by via their medical history, a neuropsychological scale, polysomnography, and a 3.0T MRI. Based on the sleep apnea-hypopnea index (AHI) scores diagnosed from polysomnography (PSG), the subjects were divided into two groups. The study group consisted of 31 untreated patients with moderate-to-severe OSAHS and the control group

consisted of 26 good sleepers (GS group). The two groups were matched according to age, sex, and education level.

Study inclusion criteria were as follows for the OSAHS group: 1) suspected of having OSAHS and were not treated in the ENT department of Zhongshan Hospital affiliated of Dalian University; 2) between 25 and 60 years of age, right-handed, completed more than 9 years of schooling; 3) AHI≥15 times/h on overnight polysomnography (PSG).For the GS control group the inclusion criteria were: 1) hospital and social volunteers whose handedness, age and education level were matched with the OSAHS group; 2) AHI<5 times/h on overnight PSG.

The study exclusion criteria were as follows: 1) respiratory diseases other than OSAHS; 2) severe hypertension, Alzheimer's disease, diabetes, and cardiovascular disease; 3) neurological diseases (epilepsy, schizophrenia and neurodegenerative diseases); 4) intracranial structural lesions (severe white matter lesions, cerebrovascular disease, brain atrophy, brain trauma, cerebral infarction, cerebral hemorrhage, and tumor); 5) a history of alcoholism, use of psychotropic substances within 1 week of study initiation; 6) metal implants, claustrophobia and other factors that would limit the acquisition of MRI data.

Polysomnography

The overnight polysomnography (PSG) examinations were performed in the sleep monitoring room in the Department of Otolaryngology, Affiliated Zhongshan Hospital of Dalian University. PSG was completed before the MRI examination. All subjects should have had at least 7 hours of sleep monitoring at night. It was required that they not take a nap on the day of monitoring, and not consume alcohol, caffeine, sedatives, hypnotics, etc. All subjects were diagnosed with OSAHS using the Alice 6 LDE diagnostic system (Philips Respironics, Murrysville, PA, USA) and other types of sleep-related diseases were excluded. The recorded items included standard EEG, electrocardiogram, sacral electromyography, electrooculogram, oral and nasal airflow, chest and abdominal movements, fingertip oxygen saturation, snoring, posture and leg movement. The sleep-related indicators calculated included the apnea-hypopnea index (AHI, events/h), apnea-hypopnea time as a percentage of total sleep time (TST in apnea-hypopnea, %), minimum oxygen saturation (minimal SaO_2, %), the mean arterial oxygen saturation (mean SaO_2,%), oxygen desaturation index (events/h), SaO_2 less than 90% of time (TST with SpO_2 <90%, min), micro-awakening index (events/h), sleep efficiency (%), total sleep time (TST, min), wake time (min), wake times, and awake index (events/h). These indexes were scored and interpreted by two senior sleep physicians according to the 2012 American Academy of Sleep Medicine (AASM) guidelines.

All subjects were assessed for the Self-Rating Anxiety Scale[27] and the Self-Rating Depression Scale.[28] We used the Epworth Sleepiness Scale[29] to assess the subjects' excessive sleepiness during the daytime. In addition, we used the Montreal Cognitive Function Scale[30] to detect screening assessment scales for cognitive impairment in eight cognitive domains: visual space/execution ability, naming, memory, attention, speech, abstraction, delayed recall, and orientation. The maximum MoCA score is 30, with a score less than or equal to 26 indicating the presence of mild cognitive impairment. These neuropsychological scales were measured by professional psychoanalysts in the psychological testing room.

MRI Data Acquisition

MRI images were obtained using a Siemens 3.0T MRI scanner with a 12-channel head coil. A T2-FLAIR MRI sequence[repetition time (TR): 8500ms, echo time (TE): 97ms, slice: 30 layers, slice thickness (ST): 4.0mm, voxel volume (voxel size, VS): 1.6 mm × 1.1 mm × 4.0 mm, matrix size (MS): 358 × 512, field of view (FOV): 280 mm × 280 mm, flip angle (FA): 150°, scanning time: 2min, 16s] was used to identify and exclude patients with intracranial structural lesions (severe white matter lesions, cerebrovascular disease, brain atrophy, brain trauma, cerebral infarction and hemorrhage, tumor).A 3D-T1WI MPRAGE sequence [TR: 1900ms, TE: 2.79ms, slice: 176, ST: 1mm, VS: 0.7mm × 0.7mm × 1.0mm, MS: 384 × 384, FOV: 259mm × 259mm, FA: 9°, scan time: 6min, 27s] was also used to collect structural brain information for further analysis. All subjects were instructed to lie comfortably on the examination table in the supine position. Foam was then used to fix the head in place to reduce movement, and earplugs were provided to reduce the effects of noise.

Image Preprocessing

First, two senior imaging diagnosticians examined the T2-FLAIR and T1WI images of each subject and marked those with poor image quality (false artifacts and incomplete images) and parenchymal lesions for exclusion. Then the T1WI images were preprocessed using the VBM8 toolbox (http://dbm.neuro.uni-jena.de/vbm) in

the SPM8 software package implemented in MATLAB 2013b (Mathworks, Natick, MA, USA). The specific steps were as follows: 1) Data format conversion: converting a DICOM format image into a NIFTI format image; 2) Segmentation: All T1WI images were segmented into gray matter (GM), white matter (WM) and cerebrospinal fluid; 3) Normalization: The GM image was registered to the Montreal Neurological Institute (MNI template) based on the DARTEL algorithm; 4) Modulation: The deviation generated in the process of standardization was corrected, which produced the final modulated GM image.

Construction of the Structural Covariance Network

According to Cao et al,[31] each brain was divided into 90 cortical and subcortical regions of interest (ROI), excluding the cerebellum, using the automatic anatomical labeling (AAL) template. The average volume of each ROI was extracted from the GM map generated by VBM. A linear regression analysis was performed for each ROI to eliminate the effects of age, gender, and mean GM total volume. The residual (corrected GM volume) of this regression was used to construct a structural covariance network.[32] Using the Pearson correlation coefficient between individual corrected GM volumes, the correlation matrix $R = [R_{ij}]$ ($I = 1 \ldots N$, $j = 1 \ldots N$, where $N = 90$) for each group was obtained. Then the diagonal elements and negative correlation of the correlation matrix were set to zero, and only the positive correlation values of the correlation matrix were retained. A specific threshold in the correlation matrix R was defined and the binary adjacency matrix $A = [A_{ij}]$ ($A_{ij} = 1$, if the absolute value of R_{ij} was greater than the threshold, otherwise, $A_{ij} = 0$) was obtained. The resulting adjacency matrix A represented a binary undirected graph G (N, E) where N is the number of nodes and E is the number of edges. The nodes represent the regions of the brain, while the edges represent undirected links between the brain regions, corresponding to non-zero elements in A.

Structural Covariance Network Analysis

The Graph Analysis Toolbox (GAT),[33] based on graph theory, was used to calculate and compare the topological properties of the structural covariance network between the OSAHS and GS groups.

Selection of Network Density Range

The absolute thresholding of the correlation matrix can result in a different number of nodes and edges in the two groups of networks and makes it very difficult for subsequent group comparisons. In order to solve this issue, a comparison between groups is set in the range of network density D, which is defined as the ratio of the existing number of edges to the maximum possible number of edges. The network density range used in this study was $0.22 \leq D \leq 0.5$. The lower limit of this range indicates the minimum density of the two groups of networks without isolated nodes ($D_{min} = 0.22$), the upper limit represents the maximum density boundary ($D_{max} = 0.5$) after which the network will approach the characteristics of the random network.[33]

Global Network Parameters

Global network parameters included the clustering coefficient (Cp), shortest path length (Lp), small-world index, transfer coefficient, global efficiency, and local efficiency. The Cp of a node is defined as the ratio of the existing number of edges between all nodes connected by a node to the maximum possible number of edges between them. The Cp of a network on the other hand is defined as the average value of the Cp of all nodes and reflects network isolation.[34] The normalized clustering coefficient is defined as $\gamma = Cp_{real}/Cp_{rand}$ where Cp_{real} represents the Cp of the actual network and Cp_{rand} represents the Cp of a random network. The shortest path length (Lp) between two nodes is defined as the minimum number of sides separating them, and the Lp of the network is defined as the average shortest path length between all node pairs within the network and generally reflects network integration.[35] The normalized shortest path length is defined as $\lambda = Lp_{real}/Lp_{rand}$, where Lp_{real} represents the Lp of the actual network and Lp_{rand} represents the Lp of a random network. The small world index σ is defined as the ratio of the normalized clustering coefficient γ to the normalized shortest path length λ ($\sigma = \gamma/\lambda$).[36] The transfer coefficient (T) is the variability of the Cp calculated at the global level; it is not the value of each node, but rather ensures elasticity by weighing the nodes with low value disproportionately.[37] Global efficiency (E_{glob}) is the reciprocal of the average of the shortest path length between node pairs in the network.[38] Similarly, local efficiency (E_{loc}) of a node is defined as the global efficiency of the subgraph that consists of its nearest neighbors, and the

E_{loc} of a network is defined as the average value of the E_{loc} of all nodes.[38]

Regional Network Parameter

The nodal degree is defined as the number of connections between a node and the rest of the network and is considered to be a measure of interaction of the node within the network.[34] The nodal betweenness is defined as the ratio of the shortest path to the total number of all shortest paths passing through a given node in the network.[34]

Network Fault Tolerance and Anti-Aggression Analysis

Fault tolerance and anti-aggression refer to the resistance of human brain networks to random faults and targeted attacks. Here, "targeted attack" means specifically deleting nodes in order of decreasing nodal degree and, "random fault" means deleting the nodes randomly in human brain networks. In order to assess network fault tolerance and anti-aggression, this study used a model that randomly or specifically deleted nodes.[35] In fault tolerance analysis, this study randomly measured the changes in the largest residual component of the network after deleting certain nodes. In order to obtain stable results, each analysis was repeated 1000 times. For the anti-aggression analysis, we measured the change in the largest residual component of the network after deleting nodes in the descending order of node degree.[39,40]

Statistical Analysis

Differences between the two groups were analyzed using the IBM SPSS statistics 20.0 software (IBM, Armonk, NY, USA). The demographic statistical parameters, neuropsychological scale scores and PSG parameters of the OSAHS group and GS group were all normally distributed. Therefore, an independent sample *t*-test was used to compare the differences between the two groups. A chi-square test was used to compare the gender of the two groups. The GAT built-in non-parametric permutation test was used to compare the network parameters of the two groups.[33,41,42] In the non-parametric permutation approach, the study redistributed the group labels to generate a correlation matrix for the random groups. The correlation matrix was then thresholded at a series of network densities to obtain a binary correlation matrix. We calculated the network properties of all binary correlation matrices and evaluated the differences between random groups for each network density. The difference between the original groups and the random groups formed a permutation map. Then, the *p*-value was calculated at the position of the permutation map based on the true difference value. We further used GAT to calculate global and local network parameters and the AUC value of the global network parameters was evaluated. Multiple comparisons were corrected for using the false discovery rate (FDR) approach. A $p < 0.05$ was considered statistically significant between the groups.

Results

Demographic Data and Clinical Data

Table 1 summarizes the clinical data of adult OSAHS patients and the GS group. We observed no significant differences for gender, age, education level, SAS score, sleep efficiency, total sleep time and awake index between the two groups ($p > 0.05$). The BMI, SDS score, ESS score, MoCA score, AHI, TST in apnea-hypopnea, lowest SpO_2, mean SpO_2, oxygen depletion index, TST with $SpO_2 < 90\%$, and arousal index showed significant differences between the two groups ($p < 0.05$).

Comparison of Global Network Metrics

In the network density of D = 0.22~0.50, the normalized clustering coefficient γ was >1, the normalized shortest path length λ was ≈1, and the small world index σ was >1 in the OSAHS group and GS group, which indicates that the structural covariance network of the two groups conforms to the characteristics of "small world" (Figure 1).

Compared with the GS group, the Cp, T, and E_{loa} of the OSAHS group were significantly increased, and the Lp was significantly increased in the narrow network density range of 0.22 to 0.24 ($p < 0.05$) (Figure 2).

The AUC analysis showed that the AUC values of the Cp ($p = 0.009$), T ($p = 0.029$), and E_{loal} ($p = 0.031$) increased significantly, and that the AUC values of σ ($p = 0.421$), γ ($p = 0.235$), λ ($p = 0.082$), Lp ($p = 0.083$), and E_{glob} ($p = 0.149$) between the two groups showed no significant differences (Figure 3).

Comparison of Regional Network Metrics

We compared nodal degree and nodal betweenness at the minimum network density between the OSAHS and GS groups. The OSAHS patients showed a decreased nodal

Table 1 Clinical Data of the OSAHS and GS Groups

Characteristics	OSAHS (n = 31)	GS (n = 26)	T (X^2)	*P*
Sex (male/female)	28/3	20/6	1.035	0.309
Age (years)	41.23±8.22	39.50±7.92	0.802	0.426
BMI (kg/m^2)	27.89±3.20	24.44±3.14	4.101	<0.001*
Education	14.71±2.83	15.42±2.69	−0.970	0.336
SAS	41.48±6.84	39.04±5.54	1.459	0.150
SDS	0.42±0.12	0.36±0.08	2.388	0.021*
ESS	10.9±6.85	7.31±4.33	2.405	0.020*
MoCA	26.00±2.07	27.58±1.39	−3.312	0.002*
Visuospatial/executive	4.58±0.76	4.27±0.87	1.430	0.157
Attention	5.35±0.98	5.92±0.39	−2.950	0.005*
Language	2.32±0.70	2.50±0.65	−0.984	0.329
Abstraction	1.84±0.45	2.00±0.00	−1.976	0.057
Delayed memory	2.94±1.39	3.88±1.31	−2.640	0.011*
Orientation	5.97±0.18	6.00±0.00	−0.914	0.364
AHI (events/h)	44.87±25.52	2.24±1.34	9.286	<0.001*
TST in apnea-hypopnea (%)	0.31±0.19	0.02±0.01	8.699	<0.001*
Minimal SpO_2 (%)	77.80±11.05	91.73±2.97	−6.732	<0.001*
Mean SpO_2 (%)	94.23±2.47	96.50±1.24	−4.491	<0.001*
Oxygen desaturation index (events/h)	46.85±31.44	2.11±2.94	7.882	<0.001*
TST with SpO_2< 90% (min)	42.25±65.04	0.20±0.54	3.600	0.001*
Micro-arousal index (events/h)	31.50±16.19	22.07±14.88	2.272	0.027*
Sleep efficiency (%)	66.67±18.83	64.89±15.95	0.380	0.706
TST (min)	341.74±104.45	326.96±88.2	0.570	0.571
Awakening index	5.14±3.58	5.41±3.30	−0.297	0.768

Notes: Data are presented as the mean ± SD. *p< 0.05 was considered statistically significant.
Abbreviations: OSAHS, obstructive apnea-hypopnea syndrome; GSs, good sleepers; BMI, body mass index; SAS, Self-Rating Anxiety Scale; SDS, Self-Rating Depression Scale; ESS, Epworth Sleepiness Scale; MoCA, Montreal Cognitive Assessment; AHI, apnea-hypopnea index; TST, total sleep time.

degree in the left angular gyrus, bilateral anterior cingulate cortex, left inferior parietal gyrus, left caudate, left pallidum and bilateral postcentral gyrus and an increased nodal degree in the left superior temporal gyrus (p<0.05, uncorrected) compared to the GS group (Figure 4A). The OSAHS patients with OSA showed a decreased nodal betweenness in the left angular gyrus, right anterior cingulate cortex, left inferior parietal gyrus, left parahippocampal gyrus, and right rolandic operculum and an increased nodal betweenness in the middle frontal gyrus, right putamen, bilateral rectus and right middle temporal gyrus (p<0.05, uncorrected) compared to the GS group (Figure 4B). Although there were no significant differences between the two groups in terms of nodal degree and nodal betweenness even after multiple comparison corrections (FDR, $p > 0.05$), OSAHS patients showed both a downward trend in nodal betweenness and noda degree in the left inferior parietal gyrus, the left angular gyrus and the right anterior cingulate cortex compared with the GS group ($p < 0.05$, uncorrected).

Difference in Network Resistance Between the OSAHS and GS Group

Analysis of network fault tolerance and anti-aggression showed that the resistance of the structural covariance network in OSAHS patients to random fault was significantly lower than that of the GS group, however, the resistance of OSAHS group to targeted attack was significantly higher than that of the GS group within 80–90% of the deleted nodes (Figure 5A). The AUC analysis (Figure 5B) further confirmed that the difference between the two groups in random failure resistance was statistically significant ($p = 0.044$), while the difference between the two groups in targeted attack resistance was not statistically significant ($p = 0.382$).

Discussion

To the best of our knowledge, this is the first study to analyze the topological changes of the structural covariance network in adult OSAHS patients. In this study, we

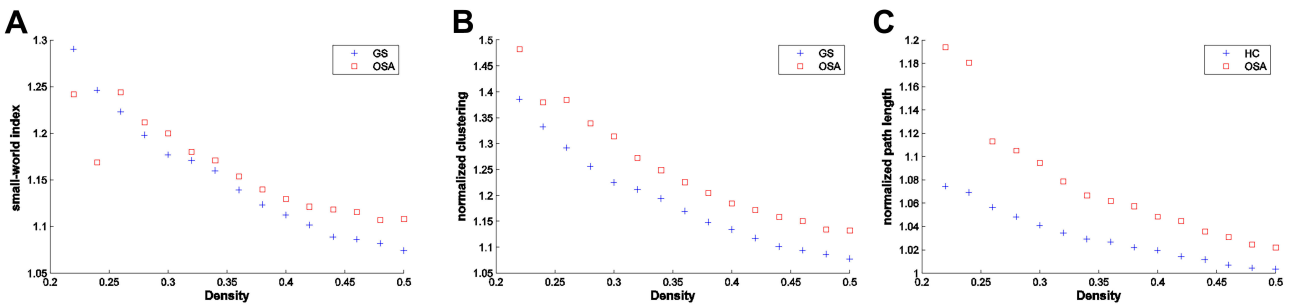

Figure 1 The small world parameters of the structural covariance network of OSAHS group and GS group. In the network density range of 0.22 to 0.50, the normalized clustering coefficient (γ) (**B**) of the OSAHS and GS groups was significantly greater than 1, the standardized shortest path length (λ) (**C**) was approximately equal to 1, and the small world index (σ) (**A**) was significantly greater than 1. These values indicate that the structure of the covariant network of the OSAHS and GS group presents typical "small world" network attributes.

found that although structural covariance networks in adult OSAHS patients conform to the characteristics of a small-world network, the topological properties of structural covariance networks are abnormal, exhibiting a significant increase in Cp, T, and E_{local}, and a significant increase in Lp in the local network density range and a high vulnerability to random faults compared with the GS group. In addition to the changes in global network parameters, regional network parameters were affected and manifested as both decreased and increased nodal betweenness/degree in OSAHS patients compared with the GS group. These results suggest that the topological properties of the structural covariance network in adult patients with moderate-to-severe OSAHS are reorganized, which provides new evidence for the neurobiological mechanism of cognitive impairment in adult patients with moderate-to-severe OSAHS from the perspective of the connectome.

OSAHS-Related Alterations in Global Network Parameters

In this study, we found that the structural covariance network of moderate-to-severe adult OSAHS patients conforms to small-world characteristics, which is consistent with previous results of the structural covariance network in children with OSAHS[26] and OSAHS resting function networks.[23–25] The small-world network has the topological advantages of a higher clustering coefficient of regular network and a shorter shortest path length of random network. The small-world network integrates the topological advantages of a regular network and a random network to ensure efficient information transmission and processing at the local and global level. This helps to promote function differentiation, function integration, and information processing and at the same time maximizes efficiency and minimizes energy consumption as well as forms the basis of cognitive function processing.[25] Our results suggest that small-world topological properties are the basic organizational components of structural brain networks.

Although small-world features exist in adult OSAHS structural covariance networks, there are significant intergroup differences in terms of multiple global network parameters. Compared with the GS group, the shortest path length in some network density ranges of OSAHS patients showed an increase and was consistent with previous studies investigating the OSAHS brain resting-state functional network.[28–30] The shortest path length of the brain network ensures the effective integrity or fast transmission of information to remote brain areas, which is considered the basis for the cognitive process.[43] Therefore, an increase in the shortest path length may reflect impairment of the functional integration of neurons across distant brain areas related to the impairment of cognitive function (measured by MoCA).

The clustering coefficient, transfer coefficient, and local efficiency are the standards used for functional separation, which can measure the ability of specialized processing in the densely connected brain regions.[34] Compared with the GS group, the OSAHS group exhibited a higher clustering coefficient, transfer coefficient, and local efficiency, which is equivalent to many closely, connected clusters and shows that the functional separation of the brain is increased and that it has a more specialized processing ability. Our findings of an increase in clustering coefficients are in contrast to the results of Chen et al.[23–25] who found that the clustering coefficients of brain functional networks in OSAHS patients were reduced, which may reflect a decrease in

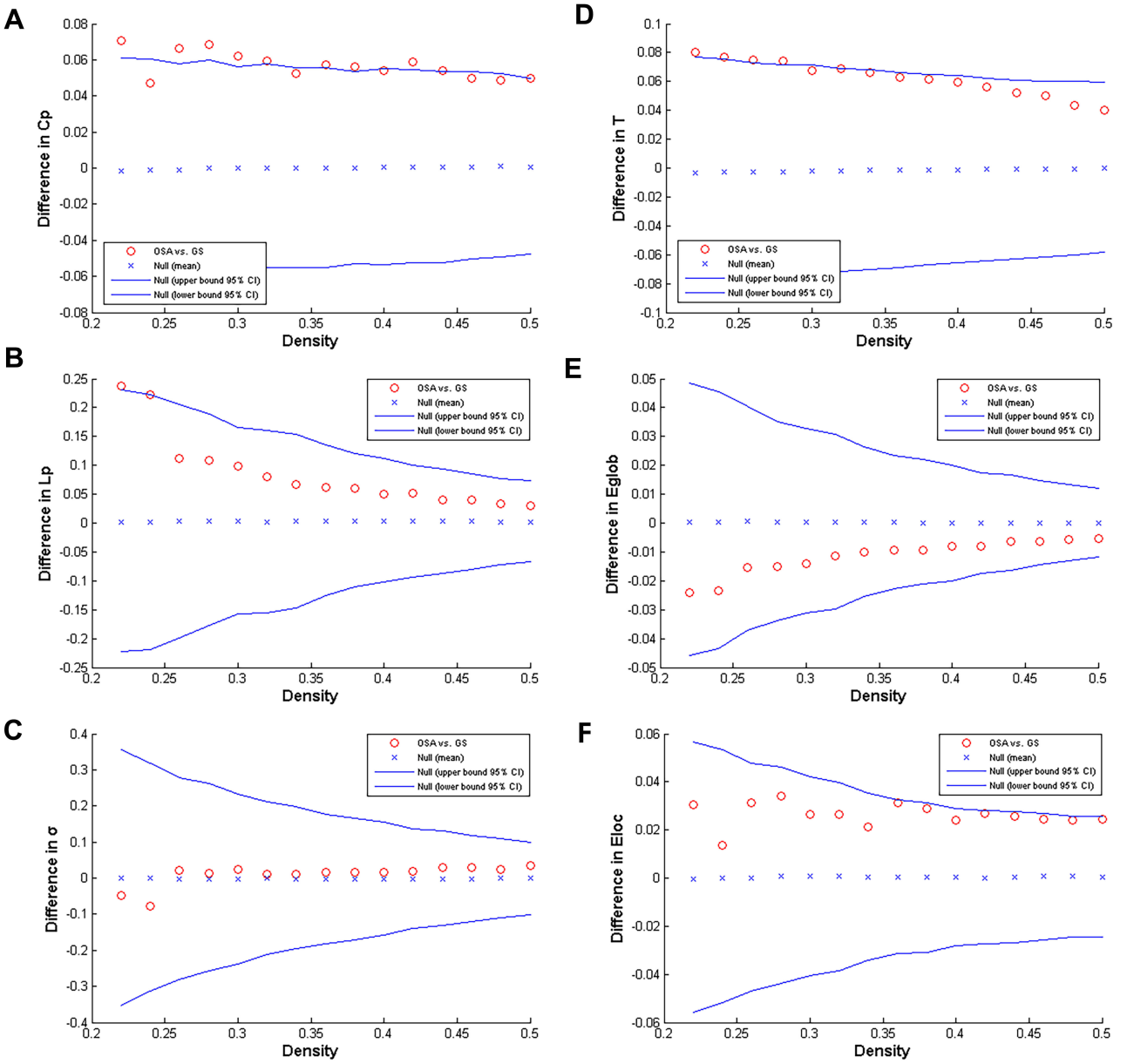

Figure 2 Inter-group differences in the global network metrics of the OSAHS and GS group in the 0.22 to 0.50 network density range. The 95% confidence interval and inter-group difference of the (**A**) clustering coefficient, (**B**) shortest path length, (**C**) small world index, (**D**) transfer coefficient, (**E**) global efficiency, and (**F**) local efficiency are shown. The red circles indicate differences between the OSAHS and GS groups; red circles outside the confidence interval indicate significant inter-group differences at the network density (p<0.05). Positive values indicate OSAHS group> GS group, negative values indicate OSAHS group <GS group.

functional network separation in compensation after an increase functional separation in the corresponding structural covariance network.[44] Likewise, the increase in local efficiency found in this study is in contrast to the findings of Luo et al who found that the local efficiency of the structural covariance network decreased in children with OSAHS.[26] This may be due to the different effects of OSAHS on the brain structure and function in children and in adults. Since the small-world model reflects the best balance between the local level specialization and the ability of global level integration via information transmission and processing, the combination of the longer shortest path length and the higher clustering in the OSAHS structural covariance network indicates that the normal balance of the brain network is disturbed and that the network tends to the regular network. Previous studies have shown that, compared with small-world networks, regular networks have lower information transmission speed and synchronization.[45] Therefore, the change in global topological properties associated with OSAHS may reflect a less ideal topological

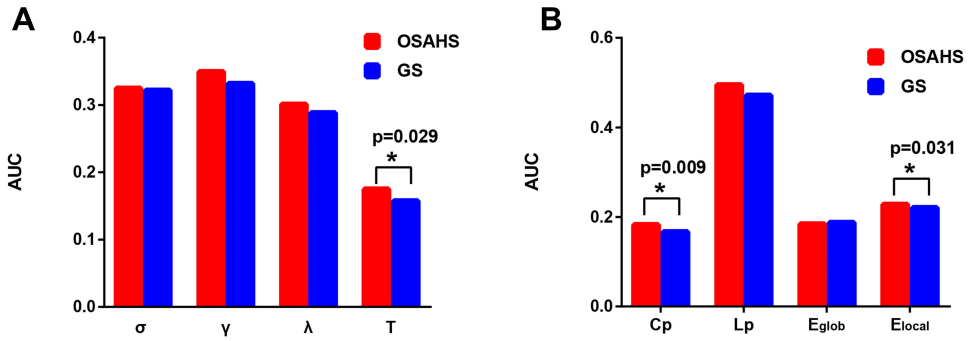

Figure 3 AUC analysis of global network metrics. (**A**) Bar graph showing the average σ, γ, λ, and T values of the OSAHS (red) and GS groups (blue). (**B**) Bar graph showing the average Cp, Lp, E_{glob} and E_{loca} values for the OSAHS (red) and GS groups (blue). *Represents p<0.05 between groups.

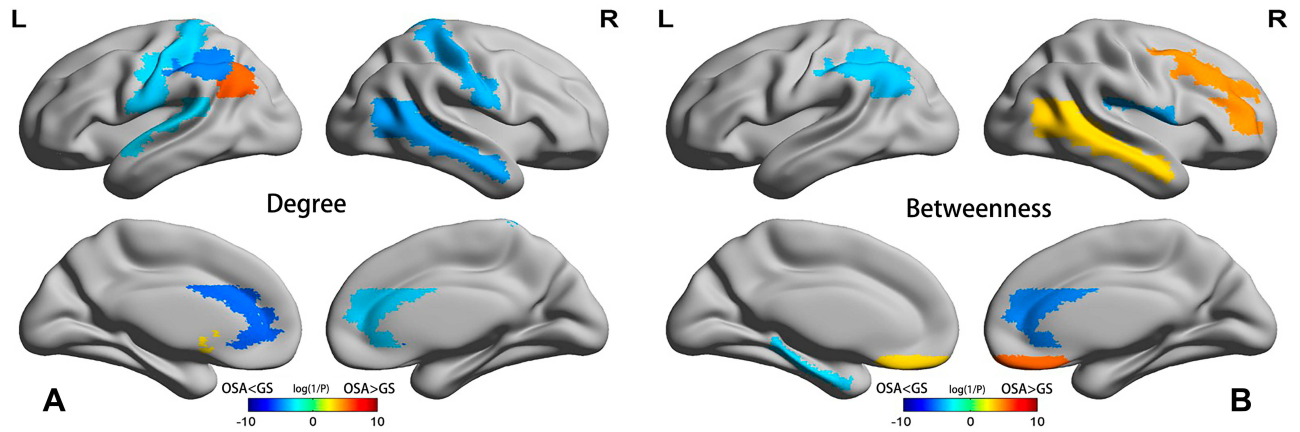

Figure 4 Differences between the OSAHS and GS groups in regional network metrics (uncorrected). Regions that showed significant differences between OSAHS and GS in nodal degree (**A**) and nodal betweenness centrality (**B**) for networks thresholded at the minimum density. The color bar indicates log(1/P). Warm colors denote regions with significantly higher nodal degree or betweenness in the OSAHS group compared with the GS group, while cool colors denote regions with significantly higher nodal degree or betweenness in the GS group compared to the OSAHS group.

organization, which provides insight for understanding the relationship between network topological properties and the neuropathological state of the disease.

OSAHS-Related Alterations in Regional Network Parameters

We found abnormal regional network parameters in multiple regions of the brain showing both decreased and increased nodal betweenness/degree in OSAHS patients compared with the GS group. Although these results were not statistically different after a correction for multiple comparisons, we should note that OSAHS patients showed both a decreased nodal betweenness and degree in the left inferior parietal gyrus, left angular gyrus and the right anterior cingulate cortex compared with the GS group, indicating that there is a downward trend in nodal betweenness and degree in these brain regions.

The inferior parietal lobule gyrus consists of the supramarginal gyrus and it is adjacent to angular gyrus. With its location at the junction between the occipital, temporal, and parietal lobes, the angular gyrus is an important interface that transmits and integrates information between different sensory modalities and processing subsystems. Abnormalities in this region have been associated with deficits in semantic processing, reading and comprehension, number processing, attention, spatial cognition, and memory retrieval.[46] Our findings regarding the decreased nodal degree and betweenness in the left inferior parietal gyrus and left angular gyrus are consistent with the results of a previous study examining the structural covariance network in children with OSAHS[26] which may further explain the low score of MoCA in OSAHS patients compared with the GS group. Additionally, since the angular gyrus is an integral part of the default mode network (DMN), our results support and confirm the concept of defects to the DMN in OSAHS proposed in previous studies.[24,47]

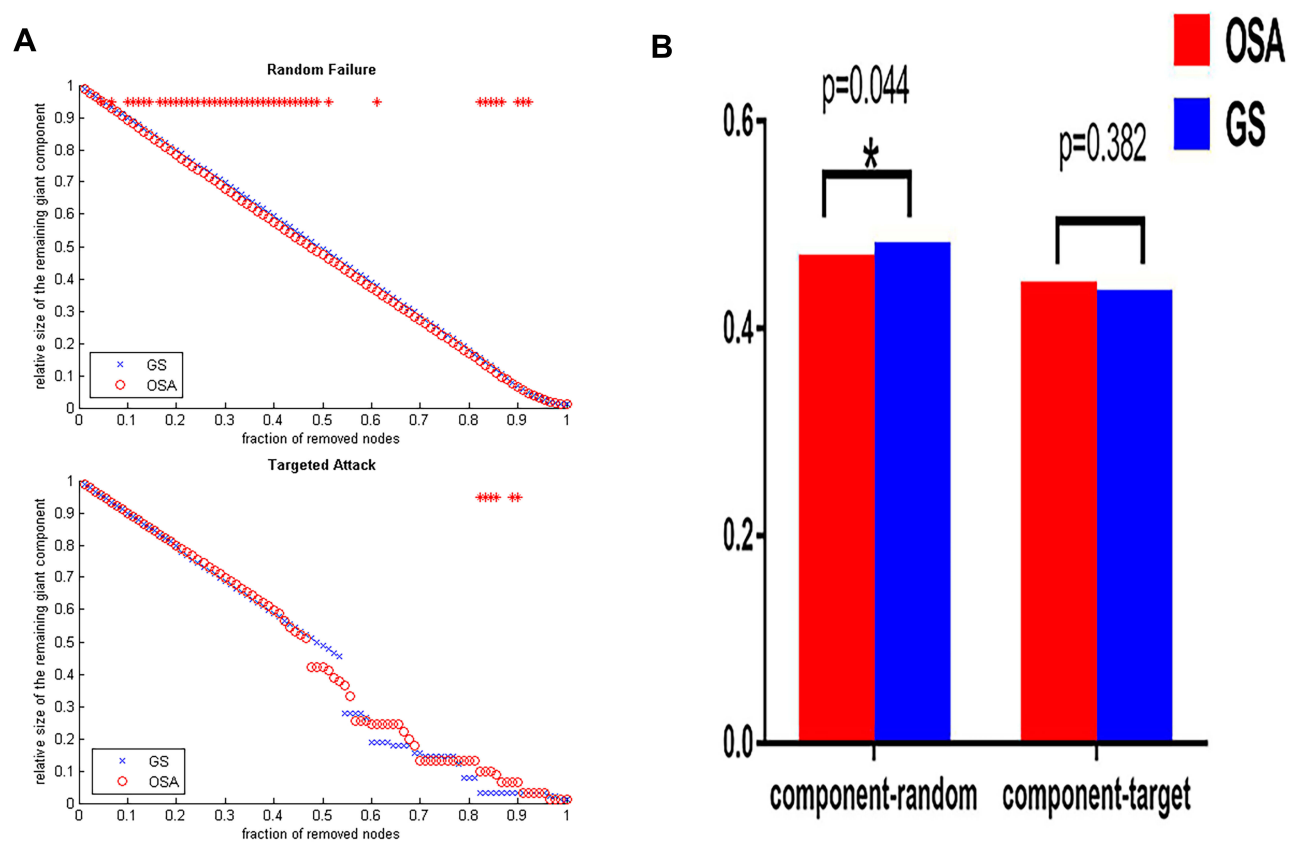

Figure 5 (**A**) The maximum remaining component size in the network after random failures and targeted attacks. The red stars indicate that the difference in the remaining maximum component of the network, between groups at which the node is deleted, is statistically significant. (**B**) Bar graph showing the average network remaining maximum component (component random) for the fault tolerance analysis and the average network remaining maximum component size (component target) for the anti-aggression analysis of the OSAHS (red) and GS (blue) groups. *Represents p<0.05 between groups.

As a part of the limbic system, the anterior cingulate cortex (ACC) is a key structure required for various activities such as autonomic nervous control, cognitive and emotional functions.[48] The ACC has also been shown to participate in central cardiovascular and respiratory control.[49] We observed decreased nodal degree and betweenness in the right ACC in OSAHS patients, which was supported by the results of a fMRI study by Chou et al.[50] who found a decreased correlation in multiple ACC functional-connected areas in patients with OSAHS compared with normal subjects. Furthermore, previous structural MRI studies have demonstrated that reduced gray matter volume[16,51] or cortex atrophy[18] occurs in the anterior cingulate gyrus, which may result in decreased nodal degree and betweenness in the ACC in the corresponding structural covariance network. The decreased nodal degree and betweenness in the right ACC may elucidate the cognitive dysfunction (measured by MoCA) and depression (measured by SDS) in OSAHS patients.

OSAHS-Related Alterations in Network Resistance

Our results confirm the high vulnerability of random faults in the structural covariance network of OSAHS patients. Previous studies have shown that small-world networks with core nodes are highly resistant to random failures and targeted attacks.[52,53] These results also showed that although the structural covariance network of OSAHS conforms to the characteristics of a small world, its resistance to random faults is reduced, which may be due to the regularization of global topology attributes associated with OSAHS. Some researchers argue that regular networks may be less resistant to pathological attacks;[54] we observed that the fault tolerance of the structural covariance network of OSAHS tends to a more regular network, which provides further evidence for this viewpoint. From the perspective of the connectome, low network fault tolerance can also provide neuroimaging evidence for OSAHS patients at high risk of neural damage and

cognitive impairment. Compared with the GS group, adult patients with moderate-to-severe OSAHS have significantly lower MoCA scores, minimal SpO_2 and mean SpO_2, higher ESS scores, TST in apnea-hypopnea, oxygen desaturation index, TST with SpO_2< 90% and the microarousal index. These results indicate that OSAHS patients are more susceptible to pathological attacks such as hypoxia, sleep disruption, anxiety, depression, and cognitive impairment, which may be related to the reduced fault tolerance of the structural covariance network of OSAHS patients.

Limitations

Despite the positive results reported here, there are various limitations to this study. First, the sample size is small, and the results of the local network parameters are uncorrected. Hence, a future study using a large sample size is needed to confirm our results. Second, cross-sectional study design was adopted for the current work, which cannot explore the dynamic development of the structural covariance network in OSAHS patients. Longitudinal studies may help elucidate abnormal dynamic patterns of disease progression. Third, this study built the structural covariance network at the group level and without the individual level network, it is impossible to explore the relationship between the network parameters and clinical variables.

Conclusions

To conclude, this study demonstrates that structural covariance networks in adult OSAHS patients are abnormal according to multiple network parameters. This result provides network-level insights into the neurobiological mechanism of cognitive impairment in adult OSAHS patients.

Ethical Statement

All procedures followed were in accordance with the National Health and Family Planning Commission "Biomedical Research Involving Human Ethics Review Approach" (the National Health Commission Order No. 11), "Helsinki Declaration" of the World Medical Association, the ethical principle of CIOMS "International Ethical Guidelines for Biomedical Research Involving Human Subjects". Informed consent was obtained from all subjects for being included in the study.

Acknowledgments

This study was supported by Dalian Medical Science Research Plan Project (No. 20181811107).

Disclosure

None of the authors have any conflict of interest to disclose.

References

1. Daulatzai MA. Evidence of neurodegeneration in obstructive sleep apnea: relationship between obstructive sleep apnea and cognitive dysfunction in the elderly. *J Neurosci Res*. 2015;93(12):1778–1794. doi:10.1002/jnr.23634
2. Young T, Peppard PE, Gottlieb DJ. Epidemiology of obstructive sleep apnea: a population health perspective. *Am J Respir Crit Care Med*. 2002;165(9):1217–1239. doi:10.1164/rccm.2109080
3. Pavlova MK, Duffy JF, Shea SA. Polysomnographic respiratory abnormalities in asymptomatic individuals. *Sleep*. 2008;31(2):241–248. doi:10.1093/sleep/31.2.241
4. Rodenstein D. Sleep apnea: traffic and occupational accidents–individual risks, socioeconomic and legal implications. *Respiration*. 2009;78(3):241–248. doi:10.1159/000222811
5. Cano-Pumarega I, Duran-Cantolla J, Aizpuru F, et al. Obstructive sleep apnea and systemic hypertension: longitudinal study in the general population: the vitoria sleep cohort. *Am J Respir Crit Care Med*. 2011;184(11):1299–1304. doi:10.1164/rccm.201101-0130OC
6. Marin JM, Carrizo SJ, Vicente E, Agusti AG. Long-term cardiovascular outcomes in men with obstructive sleep apnoea-hypopnoea with or without treatment with continuous positive airway pressure: an observational study. *Lancet*. 2005;365(9464):1046–1053. doi:10.1016/S0140-6736(05)71141-7
7. Nannapaneni S, Ramar K, Surani S. Effect of obstructive sleep apnea on type 2 diabetes mellitus: a comprehensive literature review. *World J Diabetes*. 2013;4(6):238–244. doi:10.4239/wjd.v4.i6.238
8. Yaggi HK, Concato J, Kernan WN, Lichtman JH, Brass LM, Mohsenin V. Obstructive sleep apnea as a risk factor for stroke and death. *N Engl J Med*. 2005;353(19):2034–2041. doi:10.1056/NEJMoa043104
9. Abrams B. Add alzheimer's to the list of sleep apnea consequences. *Med Hypotheses*. 2005;65(6):1201–1202. doi:10.1016/j.mehy.2005.06.014
10. Olaithe M, Bucks RS, Hillman DR, Eastwood PR. Cognitive deficits in obstructive sleep apnea: insights from a meta-review and comparison with deficits observed in COPD, insomnia, and sleep deprivation. *Sleep Med Rev*. 2018;38:39–49. doi:10.1016/j.smrv.2017.03.005
11. Martin MS, Sforza E, Roche F, Barthelemy JC, Thomas-Anterion C. group Ps: sleep breathing disorders and cognitive function in the elderly: an 8-year follow-up study. the proof-synapse cohort. *Sleep*. 2015;38(2):179–187. doi:10.5665/sleep.4392
12. Bucks RS, Olaithe M, Eastwood P. Neurocognitive function in obstructive sleep apnoea: a meta-review. *Respirology*. 2013;18(1):61–70. doi:10.1111/j.1440-1843.2012.02255.x
13. Celle S, Delon-Martin C, Roche F, Barthelemy JC, Pepin JL, Dojat M. Desperately seeking grey matter volume changes in sleep apnea: a methodological review of magnetic resonance brain voxel-based morphometry studies. *Sleep Med Rev*. 2016;25:112–120. doi:10.1016/j.smrv.2015.03.001
14. Tahmasian M, Rosenzweig I, Eickhoff SB, et al. Structural and functional neural adaptations in obstructive sleep apnea: an activation likelihood estimation meta-analysis. *Neurosci Biobehav Rev*. 2016;65:142–156. doi:10.1016/j.neubiorev.2016.03.026
15. Weng HH, Tsai YH, Chen CF, et al. Mapping gray matter reductions in obstructive sleep apnea: an activation likelihood estimation meta-analysis. *Sleep*. 2014;37(1):167–175. doi:10.5665/sleep.3330
16. Macey PM, Henderson LA, Macey KE, et al. Brain morphology associated with obstructive sleep apnea. *Am J Respir Crit Care Med*. 2002;166(10):1382–1387. doi:10.1164/rccm.200201-050OC

17. Morrell MJ, Twigg G. Neural consequences of sleep disordered breathing: the role of intermittent hypoxia. *Adv Exp Med Biol*. 2006;588:75–88.
18. Joo EY, Jeon S, Kim ST, Lee JM, Hong SB. Localized cortical thinning in patients with obstructive sleep apnea syndrome. *Sleep*. 2013;36(8):1153–1162. doi:10.5665/sleep.2876
19. O'Donoghue FJ, Briellmann RS, Rochford PD, et al. Cerebral structural changes in severe obstructive sleep apnea. *Am J Respir Crit Care Med*. 2005;171(10):1185–1190. doi:10.1164/rccm.200406-738OC
20. Baril AA, Gagnon K, Brayet P, et al. Gray matter hypertrophy and thickening with obstructive sleep apnea in middle-aged and older adults. *Am J Respir Crit Care Med*. 2017;195(11):1509–1518. doi:10.1164/rccm.201606-1271OC
21. Sporns O, Tononi G, Kotter R. The human connectome: a structural description of the human brain. *PLoS Comput Biol*. 2005;1(4):e42. doi:10.1371/journal.pcbi.0010042
22. Park B, Palomares JA, Woo MA, et al. Disrupted functional brain network organization in patients with obstructive sleep apnea. *Brain Behav*. 2016;6(3):e00441. doi:10.1002/brb3.441
23. Chen LT, Fan XL, Li HJ, et al. Disrupted small-world brain functional network topology in male patients with severe obstructive sleep apnea revealed by resting-state fMRI. *Neuropsychiatr Dis Treat*. 2017;13:1471–1482. doi:10.2147/NDT.S135426
24. Chen L, Fan X, Li H, et al. Topological reorganization of the default mode network in severe male obstructive sleep apnea. *Front Neurol*. 2018;9:363. doi:10.3389/fneur.2018.00363
25. Chen LT, Fan XL, Li HJ, et al. Aberrant brain functional connectome in patients with obstructive sleep apnea. *Neuropsychiatr Dis Treat*. 2018;14:1059–1070. doi:10.2147/NDT.S161085
26. Luo YG, Wang D, Liu K, et al. Brain structure network analysis in patients with obstructive sleep apnea. *PLoS One*. 2015;10(9):e0139055. doi:10.1371/journal.pone.0139055
27. Samakouri M, Bouhos G, Kadoglou M, Giantzelidou A, Tsolaki K, Livaditis M. Standardization of the greek version of Zung's self-rating anxiety scale (SAS). *Psychiatriki*. 2012;23(3):212–220.
28. Zung WW, Richards CB, Short MJ. Self-rating depression scale in an outpatient clinic. Further validation of the SDS. *Arch Gen Psychiatry*. 1965;13(6):508–515. doi:10.1001/archpsyc.1965.01730060026004
29. Chung KF. Use of the epworth sleepiness scale in Chinese patients with obstructive sleep apnea and normal hospital employees. *J Psychosom Res*. 2000;49(5):367–372. doi:10.1016/S0022-3999(00)00186-0
30. Smith T, Gildeh N, Holmes C. The Montreal cognitive assessment: validity and utility in a memory clinic setting. *Can J Psychiatry*. 2007;52(5):329–332. doi:10.1177/070674370705200508
31. Cao C, Liu W, Zhang Q, et al. Irregular structural networks of gray matter in patients with type 2 diabetes mellitus. *Brain Imaging Behav*. 2019. doi:10.1007/s11682-019-00070-2
32. He Y, Chen ZJ, Evans AC. Small-world anatomical networks in the human brain revealed by cortical thickness from MRI. *Cereb Cortex*. 2007;17(10):2407–2419. doi:10.1093/cercor/bhl149
33. Hosseini SM, Hoeft F, Kesler SR, Lambiotte R. GAT: a graph-theoretical analysis toolbox for analyzing between-group differences in large-scale structural and functional brain networks. *PLoS One*. 2012;7(7):e40709. doi:10.1371/journal.pone.0040709
34. Rubinov M, Sporns O. Complex network measures of brain connectivity: uses and interpretations. *Neuroimage*. 2010;52(3):1059–1069. doi:10.1016/j.neuroimage.2009.10.003
35. Bullmore E, Sporns O. Complex brain networks: graph theoretical analysis of structural and functional systems. *Nat Rev Neurosci*. 2009;10(3):186–198. doi:10.1038/nrn2575
36. Watts DJ, Strogatz SH. Collective dynamics of 'small-world' networks. *Nature*. 1998;393(6684):440–442. doi:10.1038/30918
37. Lou C, Duan X, Altarelli I, Sweeney JA, Ramus F, Zhao J. White matter network connectivity deficits in developmental dyslexia. *Hum Brain Mapp*. 2019;40(2):505–516. doi:10.1002/hbm.24390
38. Latora V, Marchiori M. Efficient behavior of small-world networks. *Phys Rev Lett*. 2001;87(19):198701. doi:10.1103/PhysRevLett.87.198701
39. Bernhardt BC, Chen Z, He Y, Evans AC, Bernasconi N. Graph-theoretical analysis reveals disrupted small-world organization of cortical thickness correlation networks in temporal lobe epilepsy. *Cereb Cortex*. 2011;21(9):2147–2157. doi:10.1093/cercor/bhq291
40. Hosseini SM, Mazaika P, Mauras N, et al. Diabetes research in children N: altered integration of structural covariance networks in young children with type 1 diabetes. *Hum Brain Mapp*. 2016;37(11):4034–4046. doi:10.1002/hbm.23293
41. Bassett DS, Bullmore E, Verchinski BA, Mattay VS, Weinberger DR, Meyer-Lindenberg A. Hierarchical organization of human cortical networks in health and schizophrenia. *J Neurosci*. 2008;28(37):9239–9248. doi:10.1523/JNEUROSCI.1929-08.2008
42. He Y, Chen Z, Evans A. Structural insights into aberrant topological patterns of large-scale cortical networks in alzheimer's disease. *J Neurosci*. 2008;28(18):4756–4766. doi:10.1523/JNEUROSCI.0141-08.2008
43. Liang XWJH, He Y. Human connectome: structural and functional brain networks (in Chinese). *Chinese Sci Bull (Chinese Ver)*. 2010;55(55):1565–1583. doi:10.1360/972009-2150
44. Niu R, Lei D, Chen F, et al. Reduced local segregation of single-subject gray matter networks in adult PTSD. *Hum Brain Mapp*. 2018;39(12):4884–4892. doi:10.1002/hbm.24330
45. Strogatz SH. Exploring complex networks. *Nature*. 2001;410(6825):268–276. doi:10.1038/35065725
46. Seghier ML. The angular gyrus: multiple functions and multiple subdivisions. *Neuroscientist*. 2013;19(1):43–61. doi:10.1177/1073858412440596
47. Peng DC, Dai XJ, Gong HH, Li HJ, Nie X, Zhang W. Altered intrinsic regional brain activity in male patients with severe obstructive sleep apnea: a resting-state functional magnetic resonance imaging study. *Neuropsychiatr Dis Treat*. 2014;10:1819–1826. doi:10.2147/NDT.S67805
48. Critchley HD, Mathias CJ, Josephs O, et al. Human cingulate cortex and autonomic control: converging neuroimaging and clinical evidence. *Brain*. 2003;126(Pt 10):2139–2152. doi:10.1093/brain/awg216
49. Frysinger RC, Harper RM. Cardiac and respiratory relationships with neural discharge in the anterior cingulate cortex during sleep-walking states. *Exp Neurol*. 1986;94(2):247–263. doi:10.1016/0014-4886(86)90100-7
50. Chou PS, Chen SC, Hsu CY, et al. medicine LCJJoc: compensatory neural recruitment for error-related cerebral activity in patients with moderate-to-severe obstructive sleep apnea. *J Clin Med*. 2019;8(7):1077.
51. Joo EY, Tae WS, Lee MJ, et al. Reduced brain gray matter concentration in patients with obstructive sleep apnea syndrome. *Sleep*. 2010;33(2):235–241. doi:10.1093/sleep/33.2.235
52. Kaiser M, Hilgetag CC. Edge vulnerability in neural and metabolic networks. *Biol Cybern*. 2004;90(5):311–317. doi:10.1007/s00422-004-0479-1
53. Achard S, Salvador R, Whitcher B, Suckling J, Bullmore E. A resilient, low-frequency, small-world human brain functional network with highly connected association cortical hubs. *J Neurosci*. 2006;26(1):63–72. doi:10.1523/JNEUROSCI.3874-05.2006
54. Achard S, Bullmore E, Friston KJ. Efficiency and cost of economical brain functional networks. *PLoS Comput Biol*. 2007;3(2):e17. doi:10.1371/journal.pcbi.0030017